Novel 1D chain Fe(III)-salen-like complexes involving anionic heterocyclic *N*-donor ligands. Synthesis, X-ray structure, magnetic, ^{57}Fe Mössbauer, and biological activity studies†

Radovan Herchel,[a] Zdeněk Šindelář,[a] Zdeněk Trávníček,*[a] Radek Zbořil[b] and Ján Vančo[a,c]

Received 26th June 2009, Accepted 10th September 2009
First published as an Advance Article on the web 2nd October 2009
DOI: 10.1039/b912676g

The iron(III) salen-type complexes [Fe(salen)(L)]$_n$ (**1–6**) involving heterocyclic *N*-donor ligands HL {HL = 1*H*-imidazole (Himz), 1*H*-tetrazol-5-amine (Hatz), 5-methyl-1*H*-tetrazole (Hmtz), 1*H*-benzimidazole (Hbimz), 1*H*-1,2,4-triazole (Htriz) and 1*H*-benzotriazole (Hbtriz)} have been prepared and characterised by elemental analysis, FT IR, CI mass and ^{57}Fe Mössbauer spectroscopies, and variable temperature magnetic measurements. Single crystal X-ray analysis of [Fe(salen)(btriz)]$_n$ (**6**) revealed a 1D chain-polymeric structure of the complex with the btriz anion as a bridging ligand. Magnetic data for all complexes were fitted using Fisher's model (for $S = 5/2$) and also using a heptanuclear closed ring model showing a weak antiferromagnetic interaction ($J \approx -1$ to -2 cm^{-1}), and moreover, molecule-based magnet properties have been observed in the case of [Fe(salen)(atz)]$_n$ (**2**). The exponential correlation between the magnetic properties (the isotropic exchange parameter J) and the basicity of the free ligands (K_b) has been found. The antiferromagnetic ordering as well as a moderate structural dissimilarity in the vicinity of iron atoms has been proved by the ^{57}Fe Mössbauer low-temperature (2 K) in-field (7 T) experiments in the case of (**2**), in which two sextets with the line intensities (3/4/1/3/4/1) have been observed. The compounds have been tested for their SOD-like activity, DNA cleavage activity, and *in vitro* cytotoxicity against two human cancer cell lines: chronic myelogenous erythroleukemia (K562) and breast adenocarcinoma (MCF7). The best result regarding the cytotoxicity has been achieved for the complex of [Fe(salen)(atz)]$_n$ (**2**), where $IC_{50} = 6.4$ μM against K562.

Introduction

The coordination compounds of iron containing the salen ligand {salen = *N*,*N*′-ethylenbis(salicylaldimato) dianion} have been known since 1933[1] and have been extensively studied due to their specific physical[2] and biological[3] properties. The great potential of the [Fe(salen)]$^+$ cation lies in its ability to catalyze redox reactions in organic syntheses[4] *e.g.* oxidation, aldol condensation and epoxidation. In addition to that, other practical applications have been recently reported, such as its use in sensing electrodes for glucose or uric acid[5] or electrochemical sensors for the determination of NO in solution.[6]

In general, there are two iron(III)-salen starting compounds, the mononuclear [Fe(salen)Cl] and dinuclear μ-oxo-bridged [{Fe(salen)}$_2$O],[7] which are the subject of the above mentioned studies, and moreover, they serve as the starting material for advanced syntheses. To put our work into context, we will summarize the chemistry of these two primary compounds with selected *N*-donor based heterocyclic compounds.

According to the Cambridge Structural Database (CSD),[8] [{Fe(salen)}$_2$O] forms adducts with pyridine (py)[9] and 1-methylimidazole,[10] in which the coordination number (c.n.) of the central atom is equal to five. Moreover, octahedral pyridine adducts of μ-hydroxo-iron(III)-salen complexes, *e.g.* [{Fe(salen)(OH)}$_2$]·2py·2H$_2$O, have also been structurally characterized.[9] Based on these facts, the formation of complexes with *N*-donor based heterocyclic ligands coordinated to the central atom of {Fe(salen)}$_2$O subunit can be excluded.

On the contrary, the reactions of [Fe(salen)Cl] with *N*-donor based heterocyclic ligands (HL) led to formation of mononuclear [Fe(salen)(H$_2$O)(HL)]Y and [Fe(salen)(HL)$_2$]Y complexes, where HL is 1*H*-pyrazole, 1*H*-imidazole or 5-phenyl-1*H*-imidazole, and Y is Cl$^-$, ClO$_4^-$, PF$_6^-$, NCS$^-$ or BPh$_4^-$,[11] however, the heterocyclic *N*-donor molecule was coordinated as a neutral ligand in all the latter-mentioned cases. In the case of the mononuclear iron(III) complex containing 1*H*-imidazole (Himz), [Fe^{III}(salen)(Himz)$_2$]ClO$_4$, the spin crossover behaviour was observed.[12]

Moreover, *N*-donor based heterocyclic compounds of the general formula HL can be utilised as anionic bridging ligands to form

[a]*Department of Inorganic Chemistry, Faculty of Science, Palacký University, Tř. 17. listopadu 12, CZ-77900, Olomouc, Czech Republic. E-mail: zdenek.travnicek@upol.cz; Fax: 00420 585634954; Tel: 00420 585634944*
[b]*Department of Physical Chemistry, Faculty of Science, Palacký University, Tř. 17. listopadu 12, CZ-77900, Olomouc, Czech Republic. E-mail: radek.zboril@upol.cz; Fax: 00420 58563 4954; Tel: 00420 58563 4947*
[c]*Department of Chemical Drugs, Faculty of Pharmacy, University of Veterinary and Pharmaceutical Sciences Brno, Palackého 1-3, CZ-612 42, Brno, Czech Republic. E-mail: vancoj@vfu.cz; Fax: 00420 54121 9751; Tel: 00420 54156 2929*

† Electronic supplementary information (ESI) available: Experimental details. CCDC reference number 737979. For ESI and crystallographic data in CIF or other electronic format see DOI: 10.1039/b912676g

more complex iron species. Such compounds are very rare and only a few are known, *e.g.* for imidazolato(1–),[13] triazolato(1–)[14] and benzotriazolato(1–)[15] anions. Introducing this kind of bridging ligand into the iron-salen compounds would lead to the formation of a novel group of polymeric iron-salen complex species with most likely interesting chemical and physical properties. The combination of the $[Fe^{III}(salen)]^+$ unit with anionic bridging ligands may result in formation of one-dimensional chains, but only two X-ray structures of such systems have been determined up to now, *i.e.* $[Fe(salen)(ac)]_n$[16] and $[Fe(salen)(dca)]_n$.[17] In these complexes, the iron atoms are linked *via* simple anions like acetato (ac) and dicyanamide (dca) as bridging ligands. The magnetic study of the latter complex showed a weak exchange interaction to be present among iron(III) centres. Both the above mentioned compounds were synthesized using [Fe(salen)Cl] as a starting material.

Herein, we report a novel approach to the preparation of polymeric iron(III)-salen-like compounds based on the fact that $[\{Fe(salen)\}_2O]$ acts as a weak base and can readily react with acids HL, such as 1*H*-imidazole (Himz), 1*H*-tetrazol-5-amine (Hatz), 5-methyl-1*H*-tetrazole (Hmtz), 1*H*-benzimidazole (Hbimz), 1*H*-1,2,4-triazole (Htriz), 1*H*-benzotriazole (Hbtriz) (Scheme 1) to form one-dimensional chains $[Fe(salen)(L)]_n$ bridged by heterocyclic aromatic *N*-donor anionic ligands. The prepared compounds have been characterized by elemental analysis, mass, infrared, electronic absorption and Mössbauer spectroscopies, and single crystal X-ray analysis. Furthermore, the magnetic and biological properties of the prepared compounds have been studied in greater detail.

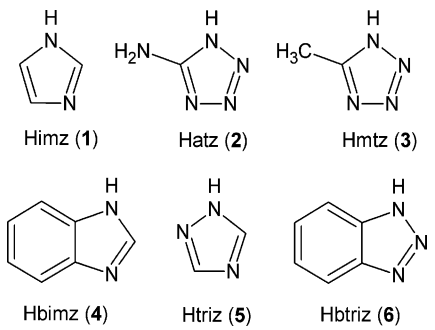

Scheme 1 Schematic representations and abbreviations used for the *N*-donor heterocyclic ligands HL. Numbers in parentheses correspond to $[Fe(salen)(L)]_n$ compounds.

Transition metals, which contain unpaired electrons in their valence shells, involved in polymeric chains often exhibit remarkable magnetic properties and might be used as precursors for the preparation of molecule-based magnets.[18] Indeed, magnetic ordering occurs for $[Fe(salen)(atz)]_n$ (**2**) below 3.5 K, probably due to the presence of hydrogen bonding among one-dimensional chains introduced through the amino group of the atz ligand. Moreover, the combination of $[Fe^{III}(salen)]^+$ units with aromatic heterocyclic ligands might result in compounds having notable biological properties. Therefore, we tested the prepared complexes for their SOD-like and DNA cleavage activities, and *in vitro* cytotoxicity. In some cases, very promising and significant results were achieved in connection with *in vitro* cytotoxicity and DNA cleavage activity.

Results and discussion

Synthesis

As a starting material for the synthesis of the iron complexes (**1–6**), a dinuclear μ-oxo-bridged complex $[\{Fe(salen)\}_2O]$ was used, prepared according to the literature.[7] This precursor was dissolved in an organic solvent (*n*-butanol or nitrobenzene) and the corresponding *N*-donor ligand HL was added in a large excess. It has been found that HL behaves as a weak acid and a general chemical equation leading to the formation of the resulting complexes can be written as follows (Scheme 2):

$$[\{Fe(salen)\}_2O] + 2\ HL \rightarrow 2\ [Fe(salen)L] + H_2O$$

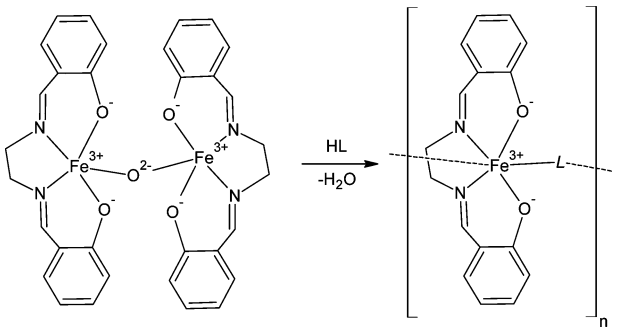

Scheme 2 Synthetic pathway for the preparation of complexes **1**, **2** and **4–6**.

The reaction mixture was heated under reflux and after cooling down, the microcrystals of $[Fe(salen)L]_n$, where HL = 1*H*-imidazole (**1**), 1*H*-tetrazol-5-amine (**2**), 1*H*-benzimidazole (**4**), 1*H*-1,2,4-triazole (**5**), 1*H*-benzotriazole (**6**), formed and were isolated.

The complex of $[Fe(salen)(mtz)]_n$ (**3**) was prepared by the reaction of $[Fe(salen)(N_3)]$ with CH_3CN under reflux. Under these conditions, the complex involving the 5-methyltetrazolide anion was formed.[19]

Structural analysis

Single crystals of $[Fe(salen)(btriz)]_n$ **6** suitable for X-ray diffraction structural analysis were obtained by slow cooling of the reaction mixture from 70 to 20 °C for seven days. The crystal data and structure refinement for **6** are given in Table 1, while selected bond distances and angles are presented in Table 2. Part of the crystal structure of complex **6** showing the crystallographically independent part of the unit cell as well as the 1D polymeric nature of the complex is depicted in Fig. 1.

The structure of **6** consists of one-dimensional $[Fe(salen)(btriz)]_n$ chains, in which deformed square-planar $[Fe(salen)]^+$ units are bridged *via* the btriz anions—Fig. S1.† The geometry of donor atoms in the vicinity of the central atom can be described as a distorted-octahedron. There are three iron(III) centres in the asymmetric unit, and surprisingly, each of the iron environments show a differently deformed coordination octahedron. However, the interatomic parameters in the vicinity of the middle iron atom differ much more than those of both lateral ones, which are more similar to each other, as can be supported *e.g.* by values of N–Fe–O angles within the polymeric chain. These angles equal

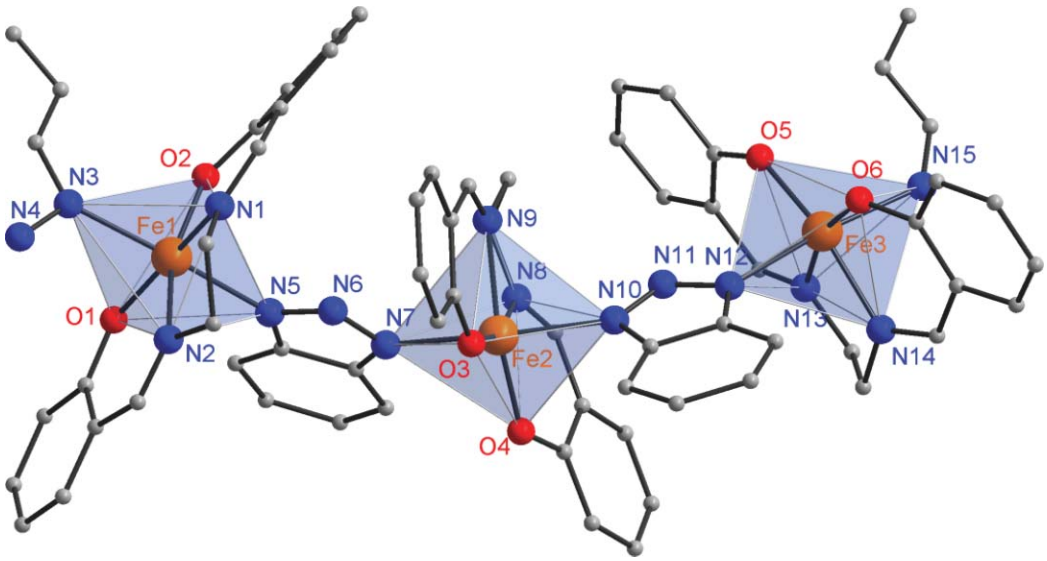

Fig. 1 Crystallographically independent part of [Fe(salen)(btriz)]$_n$ (**6**). The shaded octahedrons represent the coordination chromophore [FeN_4O_2]. The hydrogen atoms have been omitted for clarity.

Table 1 Crystal data and structure refinement for [Fe(salen)(btriz)]$_n$ (**6**)

Empirical formula	$C_{66}\ H_{54}\ Fe_3\ N_{15}\ O_6$
Formula weight	1320.79
Temperature/K	110(2)
Wavelength/Å	0.71073
Crystal system	Monoclinic
Space group	$P2_1/a$
a/Å	17.0068(2)
b/Å	19.5863(2)
c/Å	17.7921(2)
α/°	90
β/°	93.7974(10)
γ/°	90
Volume/Å^3	5913.54(11)
Z	4
Density (calculated)/Mg m^{-3}	1.484
Absorption coefficient/mm^{-1}	0.795
F(000)	2724
Crystal size/mm	0.35 × 0.30 × 0.25
θ range for data collection/°	2.59 to 25.00
Index ranges	$-18 \le h \le 20$, $-23 \le k \le 22$, $-19 \le l \le 21$
Reflections collected	49341
In dependent reflections (R_{int})	10461 (0.0199)
Data/restraints/parameters	10461/0/813
Goodness-of-fit on F^2	1.159
Final R indices [$I>2\sigma(I)$]	$R1 = 0.0283$, $wR2 = 0.0765$
R indices (all data)	$R1 = 0.0412$, $wR2 = 0.0890$
Largest diff. peak and hole/e Å^{-3}	0.504 and −0.371

Table 2 Selected bond lengths (Å) and angles (°) for [Fe(salen)(btriz)]$_n$ (**6**)

Fe1–O2	1.9037(14)
Fe1–O1	1.9115(14)
Fe1–N1	2.1250(18)
Fe1–N2	2.1274(18)
Fe1–N3	2.1650(16)
Fe1–N5	2.1662(16)
Fe2–O3	1.8987(14)
Fe2–O4	1.9082(14)
Fe2–N8	2.0986(16)
Fe2–N9	2.1283(17)
Fe2–N7	2.1323(16)
Fe2–N10	2.1756(16)
Fe3–O5	1.8942(14)
Fe3–O6	1.9066(14)
Fe3–N14	2.1110(17)
Fe3–N13	2.1326(18)
Fe3–N12	2.1608(17)
Fe3–N15	2.2240(17)
O2–Fe1–O1	109.438(59)
N1–Fe1–N2	76.487(68)
N3–Fe1–N5	173.313(62)
O3–Fe2–O4	106.413(60)
N8–Fe2–N9	77.088(67)
N7–Fe2–N10	176.021(62)
O5–Fe3–O6	107.845(60)
N14–Fe3–N13	77.045(66)
N12–Fe3–N15	174.472(62)

173.31° (Fe1), 176.92° (Fe2) and 174.14° (Fe3). Non-uniformity of each of the three iron atoms may also be evident from the crystallographic point of view, from values of O–Fe–O angles, which range from 106.4° (O3–Fe2–O4) to 109.4° (O2–Fe1–O1). Next significant changes were also observed for bond lengths between iron and axial nitrogen atoms, which range from 2.132 Å (Fe2–N7) to 2.224 Å (Fe3–N15). The one-dimensional chains are well separated and no hydrogen bonds or π–π stacking were found. Only, the weak interactions of the C–H···C and C–H···O types are present. (see Table 2).

UV-VIS, FT IR and mass spectroscopy

UV-VIS spectra were measured in the solid state and only one d–d transition at 540–580 nm was found and it may be assigned to the $^4A_2 \leftarrow {}^6A_1$ transition presuming an elongated bipyramid of the [$FeN_2O_2N'_2$] donor set. The other d–d bands were overlapped by the charge-transfer transitions.

Infrared spectroscopy confirmed the presence of the salen ligand as well as the bridging HL ligands within the complexes. The observed transitions in the range of 1626–1628 cm^{-1} may be assigned to the ν(C=N) vibration. The strong vibration of an

Table 3 ^{57}Fe Mössbauer parameters obtained at room temperature[a]

Compound	δ (mm s^{-1})	E_Q (mm s^{-1})
[Fe(salen)(imz)] (**1**)	0.394(1)	1.109(3)
[Fe(salen)(atz)] (**2**)	0.407(2)	1.518(4)
[Fe(salen)(mtz)] (**3**)	0.402(1)	1.725(3)
[Fe(salen)(bimz)] (**4**)	0.417(5)	1.35(1)
[Fe(salen)(triz)] (**5**)	0.392(5)	1.243(8)
[Fe(salen)(btriz)] (**6**)	0.397(3)	1.458(4)
[Fe(salen)(Himz)Cl][b]	0.45(2)	1.60(2)
[Fe(salen)(Himz)$_2$]ClO$_4$[c]	0.36	1.34

[a] All data are relative to natural iron foil. [b] Data taken from ref. 21. [c] Data taken from ref. 11.

azide group found in the precursor, [Fe(salen)(N_3)], disappeared in the spectrum of the final product **3**, confirming the formation of the 5-methyltetrazolide. In the case of **2**, the ν(N–H) vibration of the amine group in the 5-aminotetrazolide anion (atz) was found at 3467 cm^{-1}.

Chemical ionization mass spectroscopy (CI MS) identified the [Fe(salen)]$^+$ species (m/z = 322) and also the corresponding [HL – H]$^+$ cations of the bridging ligands, *i.e.* 69 m/z for Himz, 86 m/z for Hatz, 85 m/z for Hmtz, 119 m/z for Hbimz, 70 m/z for Htriz and 120 m/z for Hbtriz.

Mössbauer spectroscopy

The transmission ^{57}Fe Mössbauer spectra were collected at room temperature for all six compounds **1–6**. The spectra consist of the symmetric doublet with isomer shift δ ranging from 0.39 to 0.42 mm s^{-1}, which is consistent with high spin Fe(III) ions in a N/O coordination environment.[20]

The quadrupole splitting E_Q ranges from 1.11 to 1.73 mm s^{-1} (Table 3) and its relatively high value reflects the low-symmetry of the coordination sphere [FeN_4O_2]. The isomer shift for **1** is very close to values of similar compounds like [Fe(salen)(Himz)Cl][21] and [Fe(salen)(Himz)$_2$]ClO$_4$,[11] thus confirming the oxidation state as well as a type of polyhedron in the vicinity of the iron centres. The difference in the quadrupole splitting between **1** and [Fe(salen)(Himz)$_2$]ClO$_4$ can be explained by the replacement of the Himz ligand by the imz anion—Table 3.

Further, low-temperature Mössbauer spectra at T = 25 K were measured for **2** and resulted in δ = 0.516(8) mm s^{-1} and E_Q = 1.491(3) mm s^{-1}—Fig. 2. The change of the isomer shift upon cooling $\Delta\delta$ = 0.109 mm s^{-1} may be attributed to the second-order Doppler effect.[22]

In the quest to elucidate the degree of octahedron deformation in the vicinity of each of the three Fe(III) ions, and moreover, to explain a character of magnetic ordering within a 1D polymeric chain, we performed Mössbauer spectra measurements of complex **2** at 2 K in an external magnetic field of 7 T. The in-field Mössbauer spectrum of **2** including two fitted subspectra is depicted in Fig. 3. Taking into account the above-mentioned results of single crystal X-ray analysis, which clearly proved the fact that three iron atoms are present within the crystallographically independent part of the unit cell, we should have anticipated three subspectra (based on an assumption that each iron possesses a different environment).

However, the best fit was achieved in the case of two sextets with δ_1 = 0.540 mm s^{-1}, E_{Q1} = –0.475 mm s^{-1}, B_{hf1} = 42.9 T for the first sextet with area fraction 34.5% and δ_2 = 0.550 mm s^{-1}, E_{Q2} = –0.651 mm s^{-1}, B_{hf2} = 47.9 T for the second sextet. The two structurally non-equivalent Fe(III) atoms are almost indistinguishable in the spectrum and thus, they are fitted by one sextet. This sextet possibly corresponds to lateral Fe(III) atoms which are more similar to each other as proved by a single crystal X-ray analysis. The spectrum area corresponding to these "overlapped" Fe atoms is thus two-fold higher compared to the other sextet with the lower hyperfine field and quadrupole shift parameters. The second sextet should be clearly assigned to the third structurally independent Fe(III) position, *i.e.* the middle iron atom, exhibiting significantly different bond angles and generally a higher symmetry of distribution of the electric charge in the local environment of iron. The line intensities (3/4/1/3/4/1) of both sextets reflect the perfect antiferromagnetic ordering in all Fe positions, in accordance with the magnetic data.

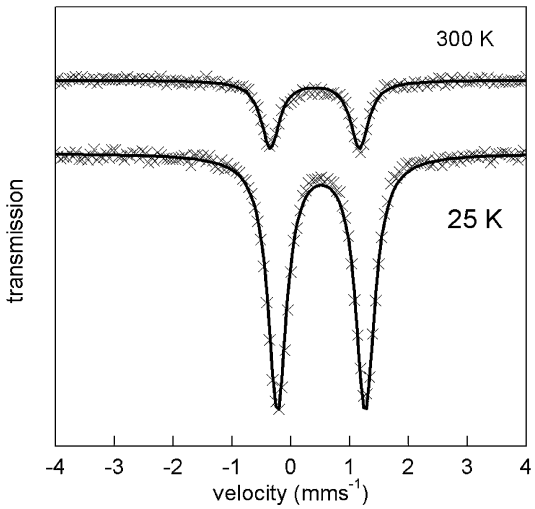

Fig. 2 ^{57}Fe Mössbauer spectra of [Fe(salen)(atz)]$_n$ (**2**) at 300 K (top) and 25 K (bottom). Cross symbols correspond to experimental data and solid lines to fitted data.

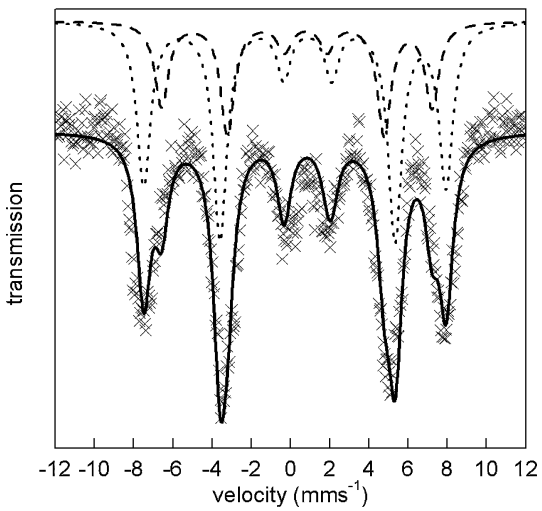

Fig. 3 ^{57}Fe Mössbauer spectra of [Fe(salen)(atz)]$_n$ (**2**) at 2 K and B = 7 T. Cross symbols correspond to experimental data and the solid line to fitted data. Dot and dashed lines correspond to fitted subspectra.

Magnetic properties

Magnetic properties of all complexes **1–6** were found to be very similar. The magnetic susceptibility calculated as $\chi_{mol} = \mu_0 M_{mol}/B$ (in SI units) increases upon cooling up to *ca.* 15 K. Below this temperature a broad maximum is observed in the range of 9–14 K and then the susceptibility is decreasing—Fig. 4.

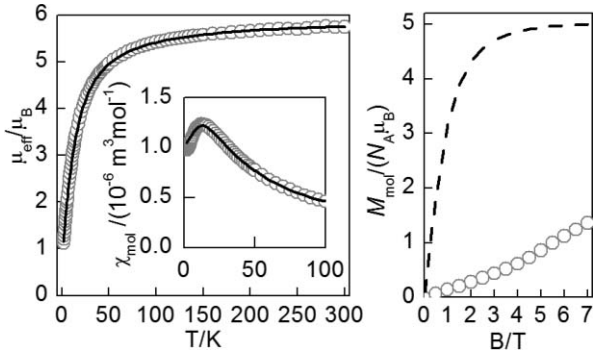

Fig. 4 Magnetic properties of [Fe(salen)(imz)]$_n$ (**1**): (left) temperature dependence of the effective magnetic moment, with the low-T region of the molar susceptibility expanded in the inset; (right) field dependence of magnetization at $T = 2.0$ K. Circles represent experimental points, solid lines represent calculated values using the best-fit parameters for a 1D chain (Table 4), the dashed line represents the Brillouin function for $S = 5/2$.

The maximum at the susceptibility *vs.* T dependence is a characteristic feature for a one-dimensional uniform chain with antiferromagnetic isotropic exchange. The room temperature values of the effective magnetic moment are in the range from 5.75 up to 5.87 μ_{eff}/μ_B and are close to the theoretical value 5.92 μ_B for an isolated iron(III) in a high-spin state with a $g = 2.0$ (Table 4).

First, the magnetic susceptibility was fitted to the one-dimensional uniform Heisenberg chain model using the following spin Hamiltonian (eq. 1)

$$\hat{H}^{chain} = -J\sum_i \vec{S}_i \cdot \vec{S}_{i+1} + \mu_B g\ \vec{B}\sum_i \vec{S}_i \qquad (1)$$

for which the well-known Fisher's formula (eq. 2) for magnetic susceptibility exists,

$$\chi_{mol} = \frac{\mu_0 N_A \mu_B^2 g^2 S(S+1)}{3kT}\frac{1+u}{1-u} \qquad (2)$$

Table 4 Spin Hamiltonian parameters resulting from fitting the magnetic data either to Fisher's model for a 1D uniform chain or to a heptanuclear ring[a]

	1D chain		Heptanuclear ring		μ_{eff}/μ_B	μ_{eff}/μ_B
	J/hc (cm^{-1})	g	J/hc (cm^{-1})	g	2 K	300 K
1	−2.17	2.01	−2.12	2.00	1.12	5.75
2	−1.89	2.01	−1.78	2.00	1.25	5.81
3	−1.80	2.02	−1.78	2.02	1.23	5.82
4	−1.79	2.01	−1.73	2.01	1.29	5.81
5	−1.53	2.00	−1.54	2.01	1.32	5.78
6	−1.59	2.01	−1.48	2.00	1.37	5.87

[a] the effective magnetic moments are calculated per one iron(III).

derived under the assumption that the local spins are treated as classical vectors,[23]

$$u = \coth\left(\frac{JS(S+1)}{kT}\right) - \left(\frac{kT}{JS(S+1)}\right) \qquad (3)$$

where u is the Langevin function (eq. 3).

The values of the isotropic exchange parameter in the 1D chain J and g-factors are summarized in Table 4. The weakest antiferromagnetic isotropic exchange was found for **5**, $J/hc = -1.53$ cm^{-1}, and the strongest for **1**, $J/hc = -2.17$ cm^{-1}. This difference reflects mostly the difference in electronic properties of the bridging ligand. In order to identify some magneto-chemical correlation, the constant of basicity K_b of the bridging ligands was used ($pK_b = 7.01$ (Himz), 8.07 (Hatz), 8.44 (Hmtz), 8.47 (Hbimz), 11.73 (Htriz) and 12.4 (Hbtriz)).[24] The exponential correlation (eq. 4) was found between J and $pK_b = -\log K_b$ with the following parameters,

$$(J/hc) = -1.53 - 42.5 \times \exp(-pK_b/1.67) \qquad (4)$$

with a correlation coefficient $R^2 = 0.99$ (Fig. 5). This simple relationship results in the conclusion that the stronger the base that is used as a bridging ligand, the stronger the antiferromagnetic exchange that is observed.

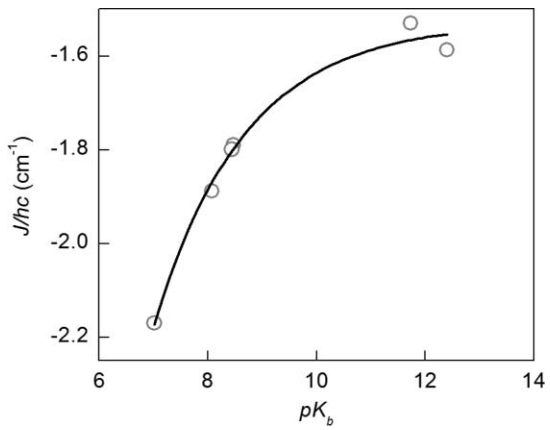

Fig. 5 The exponential correlation of the isotropic exchange *vs.* basicity of N-donor based bridging ligands. Empty circles correspond to the experimental data and the solid line corresponds to eq. 4.

The field-dependences of the molar magnetization up to $B = 7$ T at $T = 2$ K were also measured for **1–6** and show significant deviation from the Brillouin function for $S = 5/2$—Fig. 6. There is no simple analytical formula for magnetization of a 1D uniform chain as a function of the magnetic field. In order to interpret these data, the spin Hamiltonian (eq. 5) for a heptanuclear ring was postulated as

$$\hat{H}^{ring} = -J\left[\sum_i^6 \vec{S}_i \cdot \vec{S}_{i+1} + \vec{S}_7 \cdot \vec{S}_1\right] + \mu_B g\ \vec{B}\sum_i^7 \vec{S}_i \qquad (5)$$

The closed ring can mimic the magnetic properties of the 1D chain, which was utilized several times to obtain approximated analytical formulae for the magnetic susceptibility.[25]

The exchange coupling of seven Fe(III) centers, each with local spin $S_i = 5/2$, results in $(2S_i + 1)^7 = 279\,936$ magnetic states with total spins ranging from $S = 1/2$ to $S = 35/2$. For

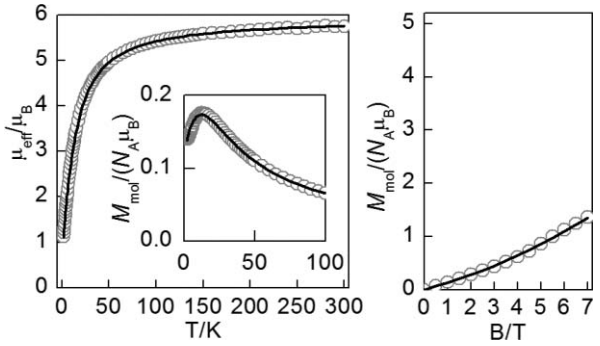

Fig. 6 Magnetic properties of [Fe(salen)(imz)]$_n$ (**1**): (left) temperature dependence of the effective magnetic moment, with the low-T region of the molar magnetization expanded in the inset; (right) field dependence of the magnetization at $T = 2.0$ K. Circles represent experimental points, solid lines represent calculated values using the best-fit parameters for a heptanuclear ring (Table 4).

the postulated spin Hamiltonian (eq. 5) it is not possible to obtain an analytical formula for the energy levels. Moreover, it is not feasible to efficiently diagonalize such large interaction matrices. To reduce the dimensions of the matrices, we have focused on the total spin symmetry principle for which the conditions (g-factors are equal for all magnetic centres and no non-isotropic terms present) are fulfilled.[26] In order to take advantage of this method, it is necessary to calculate energy values in the coupled basis set labelled as $|\alpha SM>$ using the irreducible tensor operators technique,[27] where α stands for the intermediate quantum numbers denoting the coupling path. First, only the isotropic exchange terms are involved, and the whole matrix is factorized into blocks according to the final spin quantum number S. As a result, the energies in zero magnetic field are obtained. The largest dimension of the sub-matrix is 3150 for $S = 9/2$ (Table S1†). Consequently, the energy levels in the non-zero magnetic field are calculated as $\varepsilon_i(\alpha SM) = \varepsilon_{0j}(\alpha S) + \mu_B gBM$. From the energy levels, the molar magnetization (eq. 6) can be easily calculated as

$$M_{\mathrm{mol}} = N_{\mathrm{A}}\mu_{\mathrm{B}}g\frac{\sum_i M\exp\left[-\varepsilon_i(\alpha SM)/kT\right]}{\sum_i \exp\left[-\varepsilon_i(\alpha SM)/kT\right]} \quad (6)$$

The experimental data sets (temperature dependence of the magnetization at $B = 1$ T and field dependence of the magnetization at $T = 2.0$ K) were treated simultaneously during the fitting procedure in order to unambiguously determine the fitted parameters. The results are collected in Table 4 and Fig. 6. Values of the isotropic exchange and g-factors are in good agreement with the derived values from the Fisher's formula for a 1D uniform chain. The magnetic measurement taken at $T = 2$ K for **2** revealed magnetic hysteresis with the coercive field $B_c \approx 50$ G—Fig. 7. To further magnetically characterize **2**, the zero-field cooled and the field-cooled magnetizations were measured—Fig. 8. The intercept of these curves is an indicator of the ordering temperature $T_c \approx 3.3$ K. Also, the remanent magnetization drops to zero above 3 K. The ac susceptibility measurement taken at $H_{DC} = 10$ Oe and $H_{AC} = 1.5$ Oe shows a maximum at 3.2 K in the in-phase susceptibility. Similar maximum at out-of-phase susceptibility

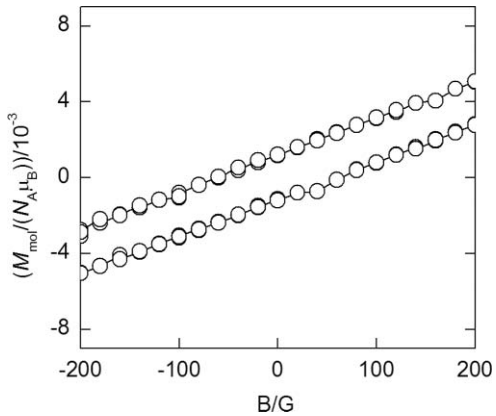

Fig. 7 The hysteresis loop of **2** measured at $T = 2$ K.

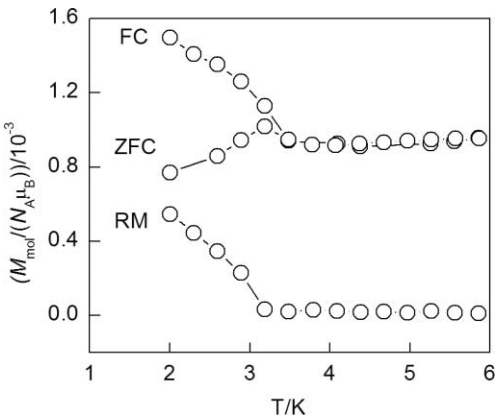

Fig. 8 Temperature variation of the field-cooled magnetization (FC), the zero-field-cooled magnetization (ZFC) and the remanent magnetization (RM) for **2** at $B = 50$ G.

is visible for the low frequencies only, which is not frequency dependent, see Fig. S2.†

To summarize, the magnetic ordering was confirmed to take place below 3.3 K for compound **2**. This exceptional behaviour in the presented series can be explained by the presence of the amine group in the bridging ligand (5-aminotetrazolide anion), which could be responsible for the hydrogen bonds among the chains in the crystal structure.

Biological activity studies

SOD-mimic activity. The superoxide dismutase (SOD) mimic activity of Fe(III)-salen complexes **1–6** was tested by a chemical method based on the competitive reaction of the tetrazolium salt XTT and the tested compound with superoxide anionic radicals produced by a saturated DMSO solution of KO_2. As a parameter of antiradical activity, the IC_{50} values were determined from the percentages of inhibition at four different concentration levels. All tested Fe(III) complexes showed moderate SOD-mimic activities in a relatively narrow range of values (IC_{50} ranges from 1.32×10^{-5} to 5.40×10^{-5} mol. dm^{-3}), reaching up to 1% of the antiradical activity of the native enzyme Cu,Zn-SOD (see Table 5), and up to 10% of the known SOD-mimic compound [Mn(salen)Cl]·H_2O, also labelled as EUK-8, used as a standard. These findings are in accordance with the published values of the SOD-mimic activity of a Fe(III) complex with the tripodal ligand

Table 5 A comparison of the SOD-mimic activity results of the complexes (**1–6**) with [Fe(salen)Cl], [{Fe(salen)}$_2$O], EUK-8 and Cu,Zn-SOD expressed in the form of IC_{50} values with the corresponding standard deviations

Complex	IC_{50} [mol. dm^{-3}]
[Fe(salen)(imz)]$_n$ (**1**)	$1.32 \pm 0.66\ 10^{-5}$
[Fe(salen)(atz)]$_n$ (**2**)	$1.89 \pm 0.38\ 10^{-5}$
[Fe(salen)(mtz)]$_n$ (**3**)	$5.40 \pm 0.30\ 10^{-5}$
[Fe(salen)(bimz)]$_n$ (**4**)	$1.96 \pm 0.09\ 10^{-5}$
[Fe(salen)(triz)]$_n$ (**5**)	$2.62 \pm 0.01\ 10^{-5}$
[Fe(salen)(btriz)]$_n$ (**6**)	$4.48 \pm 0.25\ 10^{-5}$
[Fe(salen)Cl]	$8.86 \pm 0.14\ 10^{-5}$
[{Fe(salen)}$_2$O]	$2.68 \pm 0.64\ 10^{-4}$
[Mn(salen)(Cl)]·H_2O (EUK-8)	$1.39 \pm 0.33\ 10^{-6}$
Cu,Zn-SOD	$4.80 \pm 0.29\ 10^{-7}$

Note: standard deviation calculated from three determinations.

tris(2-benzimidazolylmethyl)amine (ntb) [Fe(ntb)Cl_2]ClO_4.[28] It is also suggested in this source that the possible dismutation mechanism could be similar to that of Fe-superoxide dismutase, where a cyclic redox process occurs, in which the first stage is characterized by the reduction of Fe(III) to Fe(II) and formation of oxygen and consecutively, the second step generates a hydrogen peroxide while the Fe(II) re-oxidizes.[29] Results of mechanistic studies of interactions of a superoxide radical with [Mn(salen)(Cl)]·H_2O[30] in the chemical system similar to ours identified that at higher ratios of superoxide to complex, the oxo- and peroxo-complexes are formed. The manganese(III) complex can also undergo superoxide mediated reduction due to its specific borderline redox properties,[30] and thus, it can enter into the redox mechanism of superoxide dismutation as described above. According to the assumed facts, a similar concept is generally acceptable for Fe(III)-salen complexes mimicking some monoogygenase systems.[31] The starting compound [{Fe(salen)}$_2$O] could therefore be considered as one of the stable intermediates of the interactions between Fe(III)-salen and the superoxide radical, which may be documented by a significantly lower SOD-mimic activity of [{Fe(salen)}$_2$O]. In the case of complexes **1–6**, an interesting effect of a bridging ligand on the potentiation of SOD-mimic activity was found. It may be demonstrated by comparison of the SOD-mimic activities of complexes **1–6** with a simple non-bridging chlorido-complex [Fe(salen)Cl], in which SOD-mimic activity was found to be up to 6-times lower than that of complexes **1–6**. The effect of the bridging ligand has already been documented in the case of Fe(III)-porphyrin complexes with aromatic *N*-donor ligands and it was attributed to a beneficial π-electron effect and the soft nature of the *N*-donor ligands (*i.e.* they behave as soft-Lewis acids) in these complexes which can facilitate the superoxide interaction.[32]

The redox based mechanism of superoxide dismutation could be paradoxically one of the pathways responsible for the high cytotoxicity of the tested complexes towards tumour cell lines. There exists an accepted hypothesis that superoxide anion radicals and hydrogen peroxide are overproduced in the stage of neoplasia and at the same time play a vital role of apoptotic regulator.[33] The compounds possessing the SOD-mimic activity could therefore be responsible for the local imbalance in superoxide/hydrogen peroxide levels, leading to apoptosis of the target cells.[34]

DNA cleavage. All the Fe(III)-salen complexes **1–6** with heterocyclic *N*-ligands were tested for their nuclease activity on a model molecule of dsDNA, represented by the circular plasmid pRSET-B. The activity of the complexes to oxidatively cleave the polynucleotide chains, in the presence of a high excess of hydrogen peroxide, was monitored by gel electrophoresis, which allowed qualitative and quantitative evaluation of different forms of the modified DNA. The quantitative parameter of total DNA cleavage was calculated as the percentage of the integrated density of cleaved forms (OC-form + 2 × L-form) from the sum of integrated densities of all identified forms of DNA (CCC-form + OC-form + 2 × L-form). For a better understanding of the Fe(III)-salen complex–DNA interaction, the actual final concentration in the tested system was recalculated to express the molar ratio of the tested compound to one base pair (bp) of plasmid DNA.

Table 6 DNA cleavage by the complexes (**1–6**), [Fe(salen)Cl], [{Fe(salen)}$_2$O] and EUK-8 in the presence of ascorbic acid at the 1:1 base pair (bp) molar ratio[a]

Compound	D_I/percentage of CCC-form	D_{II}/percentage of OC-form	DNA cleavage (%)
pRSET-B	3116/58.8	380/7.2	10.9
[Fe(salen)(imz)]$_n$ (**1**)	3297/59.3	734/13.2	18.2
[Fe(salen)(atz)]$_n$ (**2**)	1023/51.9	753/38.2	42.4
[Fe(salen)(mtz)]$_n$ (**3**)	1293/55.4	1040/44.6	44.6
[Fe(salen)(bimz)]$_n$ (**4**)	4234/55.5	1180/15.5	21.8
[Fe(salen)(triz)]$_n$ (**5**)	3836/49.1	2082/26.7	35.2
[Fe(salen)(btriz)]$_n$ (**6**)	3772/50.0	1663/22.0	30.6
[Fe(salen)Cl]	922/37.1	1563/62.9	62.9
[{Fe(salen)}$_2$O]	608/34.4	1158/65.6	65.6
[Mn(salen)(Cl)]·H_2O (EUK-8)	1440/56.3	1116/43.7	43.7
control	3153/79.8	292/7.4	10.8

[a] D_I, D_{II}—integrated density of CCC-form and OC-form respectively; the percentage of DNA cleavage was calculated by the following equation: DNA cleavage = $D_{II}/(D_I + D_{II})$.

In the chemical system including the hydrogen peroxide, only an insignificant increase of the DNA cleavage was identified, thus excluding the "peroxidase-like" pathway connected with the formation of the ferryl (Fe^{4+}) species from the cleavage of DNA.

On the other hand, in the system with the hydrogen peroxide supplemented with L-ascorbic acid as reducing agent, all the tested complexes showed a significant increase in DNA cleavage on both tested concentration levels up to 63% (See Table 6, Table 7, Fig. 9, and ESI† for additional results).

Moreover, at relatively high concentration (120 μM, 5:1 bp molar ratio), the formation of small fragments of DNA was observed. At both concentration levels, the DNA cleavage caused by the simple [Fe(salen)Cl] and the starting complex [{Fe(salen)}$_2$O] used for the synthesis of complexes **1–6** was significantly higher than that of the complexes **1–6**. On the other hand, the known manganese based SOD-mimic compound EUK-8, cleaved the DNA on a similar level as compared with the complexes **1–6**.

The mechanism of DNA-cleavage is based on the well-known hypothesis of sequence non-specific interaction of the soluble cationic coordination unit [Fe(salen)]$^+$ with the phosphate moieties of double helical DNA,[35] reduction of Fe(III) and Fenton reaction-mediated production of reactive oxygen species that are able to cleave the polynucleotide chains, probably at the C1′ or C4′ position of the adjacent deoxyribose moiety.[36]

***In vitro* cytotoxicity.** The *in vitro* cytotoxicity of the complexes **1–6** against K562 and MCF7 human cancer cell lines was

Table 7 The DNA cleavage by the complexes (**1–6**), [Fe(salen)Cl], [{Fe(salen)}$_2$O] and EUK-8 in the presence of ascorbate at 5:1 bp molar ratio[a]

Compound	D_I/percentage of CCC-form	D_{II}/percentage of OC-form	DNA cleavage (%)
[Fe(salen)(imz)]$_n$ (**1**)	2963/45.6	1929/29.7	39.4
[Fe(salen)(atz)]$_n$ (**2**)	266/22.6	457/38.9	63.3
[Fe(salen)(mtz)]$_n$ (**3**)	482/37.7	795/61.8	62.1
[Fe(salen)(bimz)]$_n$ (**4**)	3510/41.8	2467/29.4	41.3
[Fe(salen)(triz)]$_n$ (**5**)	2706/34.6	3294/42.1	54.9
[Fe(salen)(btriz)]$_n$ (**6**)	3162/40.0	2905/36.8	47.9
[Fe(salen)Cl]	498/30.2	1152/69.8	69.8
[{Fe(salen)}$_2$O]	120/19.4	266/42.4	68.6
[Mn(salen)(Cl)]·H_2O (EUK-8)	1619/54.9	1330/45.1	45.1
Control	2863/85	171/5.1	5.7

[a] D_I, D_{II}—integrated density of CCC-form and OC-form respectively; the percentage of DNA cleavage was calculated by the following equation: DNA cleavage = $D_{II}/(D_I + D_{II})$.

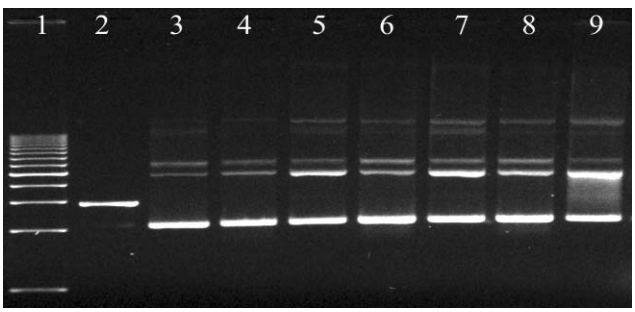

Fig. 9 An example of an electrophoreogram showing the effect of concentration on the oxidative cleavage of plasmid DNA in the presence of ascorbic acid. Lane (1) ladder 1kbp, (2) linearized plasmid (pure L-form, cleaved by HInd III endonuclease), (3) supercoiled plasmid DNA (majority of CCC-form), (4) complex **1** at the molar ratio 1:1 bp, (5) complex **1** at the molar ratio 5:1 bp, (6) complex **4** at the molar ratio 1:1 bp, (7) complex **4** at the molar ratio 5:1 bp, (8) complex **6** at the molar ratio 1:1 bp, (9) complex **6** at the molar ratio 5:1 bp.

determined by a calcein acetoxymethyl (AM) assay. The activity was expressed as the concentration (in μM) of the compounds at which tumour cell growth showed 50% inhibition (IC_{50}). The results of the testing are summarized in Table 8.

The *in vitro* cytotoxic properties can be evaluated by comparison of values found for the Fe(III) complexes against the starting compounds, *i.e.* [{Fe(salen)}$_2$O] and free HL ligands. It may be noted that all the tested complexes show significant *in vitro* cytotoxicity against both K562 and MCF7 cell lines. The most promising cytotoxity has been found in the case of complex **2** involving the 5-aminotetrazolide anion (atz). In many cases, the effect of iron on the hydrogen peroxide toxicity was explained by the initiation of the Fenton reaction. The continuously broadened outlook for the mechanisms of cytotoxicity mediated by Fe(III) complexes showed, however, more sensitive and more specific pathways mediated by the activation of specific genes.[37] Indeed, the activation of the mitochondrial pathway of apoptosis was discovered for [Fe(salen)Cl] and [Fe(III)(saloph)(H_2O)Cl] complexes.[38] The hypothesis of the multimodal effect of iron on the hydrogen peroxide cytotoxicity was also supported by ref. 39 who found

Table 8 The cytotoxicity of the studied compounds, expressed as IC_{50} values (μM), assessed by a calcein AM assay for the two human cancer cell lines[a]

	Values of IC_{50} (μM) for the complex/free ligand	
	K562	MCF7
[Fe(salen)(imz)]$_n$ (**1**)	9.8 ± 1.8/>100	23.7 ± 3.6/>100
[Fe(salen)(atz)]$_n$ (**2**)	6.4 ± 1.2/>100	13.1 ± 2.1/>100
[Fe(salen)(mtz)]$_n$ (**3**)	11.2 ± 2.1/>100	20.6 ± 3.1/>100
[Fe(salen)(bimz)]$_n$ (**4**)[b]	>1/>50	>1/>50
[Fe(salen)(triz)]$_n$ (**5**)	10.1 ± 1.7/>100	18.3 ± 2.9/>100
[Fe(salen)(btriz)]$_n$ (**6**)	10.9 ± 1.9/>100	16.9 ± 2.8/>100
[Fe(salen)Cl]	—/—	22.0 ± 0.7[c]/—
oxaliplatin	9.0	18.0
cisplatin	5.0	11.0

[a] K562–chronic myelogenous erythroleukemia, MCF7–breast adenocarcinoma. [b] The complex could not be tested in the desired concentration range owing to the limited solubility in the testing medium. [c] The value was obtained by an MTT test and taken from Ref. 40.

that the efficient hydroxyl radical scavengers had no significant effect on the iron influenced hydrogen peroxide toxicity in the LLC-PK_1 cells and deduced that other reactive iron-oxygen species, such as ferryl (Fe^{4+}), perferryl (Fe^{5+}) and various other forms are probably responsible for the cytotoxic effect. Although the indirect dependence of the cytotoxicity of [Fe(salen)Cl], [Fe(saloph)Cl] and [Fe(salnaphen)] complexes, where H_2salnaphen stands for Schiff base derived from salicylaldehyde and naphthalene-2,3-diamine, against MFC7 cells on the *in vitro* DNA-cleavage results has already been described,[40] no such effect could be found in the case of our experiments.

Conclusions

In this work, six novel iron(III)-salen complexes with *N*-donor aromatic heterocyclic bases (HL) were prepared and characterized by a broad spectrum of physical techniques. X-ray analysis revealed a one-dimensional molecular structure, in which the anionic base acts as the bidentate bridging anionic ligand (L). Mössbauer spectroscopy and magnetic measurements showed that iron(III) centres are in the high-spin state over the whole temperature interval and the isotropic exchange among them is in the range from –1 to –2 cm^{-1}. An exponential correlation was found between the magnetic properties (the isotropic exchange parameter *J*) and the electronic properties of the bridging ligand (basicity K_b). Moreover, the [Fe(salen)(atz)]$_n$ **2** revealed magnetic properties corresponding to a molecule-based magnet.

Further, biological activity studies revealed the great potential of the prepared complexes to behave as promising anti-tumour species, as proved by *in vitro* tests against K562 and MCF7 human cancer cell lines. All tested compounds exhibited moderate SOD-mimic activity, reaching up to 1% of Cu,Zn-SOD and up to 10% of a known SOD-mimic compound [Mn(III)(salen)Cl]·H_2O (EUK-8), used as a standard. Both *in vitro* methods of antioxidant activity (*i.e.* SOD-mimic activity and DNA cleavage) suggested the possible mechanism of reactive oxygen species related to cytotoxicity, connected either with the Fe(III) complex mediated imbalance in the superoxide/hydrogen peroxide ratio or Fenton-like DNA-cleavage, or the formation of other reactive species

{*e.g.* ferryl (Fe^{4+}) or perferryl (Fe^{5+}) species} leading to apoptosis of target cancer cells.

Experimental

All chemicals purchased were chemically pure and were of analytical reagent grade and used without further purification. Elemental analyses (C, H, N) were performed on a EA-1108 Analyzer Fisons Intrument. UV-VIS spectra were recorded on a Perkin-Elmer Lambda 40 UV/VIS spectrometer in the solid state using the nujol technique in the range of 9000–30 000 cm^{-1}. Infrared spectra of the complexes were recorded on a Perkin-Elmer SPECTRUM One FT-IR spectrometer using KBr pellets in the range 400–4000 cm^{-1}, and on a ThermoNicolet NEXUS 670 FT-IR spectrometer using polyethylene discs in the range 200–600 cm^{-1}. The transmission ^{57}Fe Mössbauer spectra were collected using a Mössbauer spectrometer in a constant acceleration mode with a ^{57}Co(Rh) source. The measurements were carried out at room temperature (for all complexes **1–6**). Complex **2** was also investigated at 2 K in an external magnetic field of 7 T applied parallel to the γ-ray propagation. CI mass spectra of the complexes were obtained in the solid state using a direct probe on Thermo-Electron Polaris Q mass spectrometer with an ion trap analyzer. Isobutane was used as the ionization gas. The compounds were heated in a temperature program from 40–450 °C. Electron energy 10 eV was applied. The mass monitoring interval was 50–1000 m/z. Variable temperature (T = 2–300 K, B = 1 T) and variable magnetic field (B = 0–7 T, T = 2 K) magnetisation measurements on polycrystalline samples were carried out with a MPMS XL-7 Quantum Design SQUID magnetometer. Experimental data were corrected for the diamagnetism of the constituent atoms by using Pascal's Tables constants and for the diamagnetism of the sample holder.

Synthesis

The compounds of the general formula $[Fe(salen)(L)]_n$ (**1**, **2** and **4–6**) were prepared according to the general procedure: an excess of the heterocyclic *N*-donor base HL (4 mmol) was added to a *n*-butanol (80 mL) solution of $[(Fe(salen))_2O]$ (0.10 g, 0.15 mmol) prepared according to ref. 9. The mixture was heated to the boiling temperature and 10–20 mL of solvent was evaporated. After cooling of the resulting solution to room temperature, microcrystals were precipitated, filtered off and washed with a small amount of hot *n*-butanol and diethyl ether.

The compound $[Fe(salen)(mtz)]_n$ (**3**) was prepared by heating the reaction mixture of 0.1 g $[Fe(salen)(N_3)]^2$ with acetonitrile (50 mL) under reflux for 24 h. As a result, the 5-methyltetrazolide anion was formed.[19] After cooling down the resulting mixture to ambient temperature, the microcrystals of product **3** formed, were isolated by filtration and washed with small amounts of acetonitrile and diethyl ether.

$[Fe(salen)(imz)]_n$ (1). Yield: 0.08 g 70% (based on Fe). (Found: C, 58.06; H, 4.01; N, 14.10. $FeC_{19}H_{17}N_4O_2$ requires C, 58.63; H, 4.40; N, 14.40%); λ_{max}(nujol)/nm: 572; ν_{max}(KBr)/cm^{-1}: 1627, 1599, 1542, 1467, 1446, 1341, 1304, 1085, 760, 616, 419; CI-MS (m/z, amu): 322 (100%, $[Fe(salen)]^+$), 69 (10, H_2imz^+).

$[Fe(salen)(atz)]_n$ (2). Yield: 0.09 g 74% (based on Fe). (Found: C, 50.24; H, 4.04; N, 24.02. $FeC_{17}H_{16}N_7O_2$ requires C, 50.27; H, 3.97; N, 24.17%); λ_{max}(nujol)/nm: 576; ν_{max}(KBr)/cm^{-1}: 3467, 2918, 1630, 1547, 1468, 1444, 1392, 1335, 1291, 1150, 906, 797, 158, 620; CI-MS (m/z, amu): 322 (100%, $[Fe(salen)]^+$), 86 (20%, H_2atz^+).

$[Fe(salen)(mtz)]_n$ (3). Yield: 0.08 g 67% (based on Fe). (Found: C, 53.08; H, 4.26; N, 21.17. $FeC_{18}H_{17}N_6O_2$ requires C, 53.35; H, 4.29; N, 20.74%); λ_{max}(nujol)/nm: 558; ν_{max}(KBr)/cm^{-1}: 1627, 1598, 1546, 1469, 1445, 1391, 1336, 1149, 907, 799, 758, 621; CI-MS (m/z, amu): 322 (100%, $[Fe(salen)]^+$), 85 (42, H_2mtz^+).

$[Fe(salen)(bimz)]_n$ (4). Yield: 0.09 g 70% (based on Fe). (Found: C, 62.45; H, 4.76; N, 12.55. $FeC_{23}H_{19}N_4O_2$ requires C, 62.89; H, 4.36; N, 12.75%); λ_{max}(nujol)/nm: 540; ν_{max}(KBr)/cm^{-1}: 1627, 1599, 1543, 1467, 1446, 1336, 1298, 751, 618, 420; CI-MS (m/z, amu): 322 (16%, $[Fe(salen)]^+$), 119 (100, H_2bimz^+).

$[Fe(salen)(triz)]_n$ (5). Yield: 0.09 g 75% (based on Fe). (Found: C, 55.41; H, 4.11; N, 17.62. $FeC_{18}H_{17}N_5O_2$ requires C, 55.26; H, 4.38; N, 17.90%); λ_{max}(nujol)/nm: 564; ν_{max}(KBr)/cm^{-1}: 1628, 1599, 1542, 1466, 1447, 1339, 1303, 757, 618, 421; CI-MS (m/z, amu): 322 (100%, $[Fe(salen)]^+$), 70 (62, H_2triz^+).

$[Fe(salen)(btriz)]_n$ (6). Yield: 0.08 g 61% (based on Fe). (Found: C, 59.50; H, 4.05; N, 15.20. $FeC_{22}H_{18}N_5O_2$ requires C, 60.02; H, 4.12; N, 15.91%); λ_{max}(nujol)/nm: 540; ν_{max}(KBr)/cm^{-1}: 1627, 1599, 1543, 1468, 1446, 1336, 1298, 907, 751, 618, 423; CI-MS (m/z, amu): 322 (100%, $[Fe(salen)]^+$), 120 (15, H_2btriz^+).

Single crystal X-ray structure studies

X-ray measurements on the selected crystal of complex **6** was performed on an Oxford Diffraction Xcalibur™2 equipped with a Sapphire2 CCD detector using Mo-K_α radiation at 110 K. The CrysAlis program package (version 1.171.32.11, Oxford Diffraction) was used for data collection and reduction. The molecular structure of **6** was solved by direct methods SHELX-97 and all non-hydrogen atoms were refined anisotropically on F^2 using the full-matrix least-squares procedure SHELXS-97 with weight: $w = 1/[\sigma^2(F_o)^2 + (0.047P)^2 + 3.122P]$, where $P = (F_o^2 + 2F_c^2)/3$.[41] All H atoms of **6** were found in differential maps of electron density and their parameters were refined using the riding model with the C–H distance of 0.950 (CH), and 0.990 (CH_2) Å, respectively, and with $U_{iso}(H) = 1.2\ U_{eq}(C)$. Additional calculations were performed using the DIAMOND program.[42] Crystal data and structure refinement of **6** are summarized in Table 1 while selected interatomic parameters are given in Table 2.

Cytotoxicity testing

The cytotoxicity of the free ligands and their iron(III) complexes **1–6** were tested *in vitro* by a calcein AM assay against the following human cancer cell lines: chronic myologenous leukemia K562 and breast adenocarcinoma cell line MCF7. The cells were treated with a solution of the tested compound for 72 h at 37 °C, 5% CO_2; in the range of 0.41–100 μM for **1–3** and **5–6**; in the range of 0.1–50 μM for **4**. Further details regarding the biological activity testing are detailed in ref. 43. The IC_{50} values are represented by the arithmetic mean of three values.

SOD-mimic activity testing

The SOD-mimic activities were measured by an indirect method based on the competitive reaction of the tested compounds with XTT dye [sodium 5,5′-(5-(phenylcarbamoyl)-2*H*-tetrazole-3-ium-2,3-diyl)bis(4-methoxy-2-nitrobenzenesulfonate)] with a saturated DMSO solution of potassium superoxide (KO_2). Generally, the interactions of XTT dye with superoxide anion radical, led to the formation of orange XTT-formazane. The scavengers of superoxide radicals inhibit the formation of XTT-formazane and the percentage of inhibition of this reaction was determined by spectroscopic measurements at 480 nm. The IC_{50} values, calculated from a linearized logarithmic curve of the concentration dependence of the percentage of inhibition, represent the concentrations of tested Fe(III) complexes which reduced formazane formation by 50%.

Required amounts of DMSO solutions of the tested compounds to provide 500, 100, 50, 25 and 10 μM solutions were added to 1.25 ml of 10 mM potassium phosphate buffer (pH 7.4) and 50 μl of XTT solution in DMSO was added. The resulting solution was mixed thoroughly. The reaction was started by addition of 100 μl of saturated KO_2 solution in DMSO and the absorbance at 480 nm was measured against the blank prepared without addition of XTT dye (value *A*). The same procedure was used to prepare the control sample without the tested Fe(III) complexes and the absorbance at 480 nm was measured against the solution of XTT before the reaction with superoxide (value *B*). All samples were incubated for 30 min at laboratory temperature. Three samples of each concentration level of all Fe(III) complexes were tested ($n = 3$). Percentages of inhibition (%*INH*) values were determined according to the eq. 7. The IC_{50} values were calculated from a linearized logarithmic curve of the concentration dependence of the percentage of inhibition and represent the concentrations of tested Fe(III) complexes which reduced the formazane formation to 50%.

$$\%\,INH = 100 \cdot \left(1 - \frac{A}{B}\right) \tag{7}$$

DNA cleavage studies

Supercoiled plasmid DNA, pRSET-B (2939 bp, 1811,9 kDa), was obtained from Invitrogen, Netherlands, solubilized in TE buffer (10 mM TRIS, 1 mM EDTA, pH = 8.0, 582 μg/ml). Supercoiled plasmid, pRSET-B (0.5 μl per reaction) was mixed with various concentrations of Fe(III)-salen complex (in different experiments, the various final concentrations of Fe(III)-salen complex to one base pair (bp) of dsDNA were used, usually 1:1 to 5:1 bp) in the presence and absence of the reducing agent L-ascorbic acid in TE buffer. Reaction mixtures were incubated at 37 °C for 1 h and then analyzed by 0.8% agarose gel electrophoresis and detected with ethidium bromide staining. The electrophoreogram was analyzed by the software AlphaEaseFC version 4.0.0.34 (Alpha Innotech, USA) and the relative percentages of circular (CCC), one strand nicked (OC), and linear (L) forms were evaluated.

Acknowledgements

We acknowledge the financial support from the Czech Ministry of Education, Youth and Sports (MSM6198959218, 1M6198959201) and the Academy of Sciences of the Czech Republic (KAN115600801). Authors would like to thank Mrs. Dita Parobková for the cytotoxicity testing.

Notes and references

1 P. Pfeiffer and T. Tsumaki, *Ann. Chem.*, 1933, 83.
2 M. Gullotti, L. Casella, A. Pasini and R. Ugo, *J. Chem. Soc., Dalton Trans.*, 1977, 339; K. S. Murray, *Coord. Chem. Rev.*, 1974, **12**, 1; H. Noglik, D. W. Thompson and D. V. Stynes, *Inorg. Chem.*, 1991, **30**, 4571; L. Gaillon, N. Sajot, F. Bedioui, J. Devynck and K. J. Balkus, *J. Electroanal. Chem.*, 1993, **345**, 157.
3 Y. Shapira, M. T. Liu, S. Foner, C. E. Dube and P. J. Bonitatebus, Jr., *Phys. Rev. B: Condens. Matter Mater. Phys.*, 1999, **59**, 1046; T. W. Failes and T. W. Hambley, *J. Inorg. Biochem.*, 2007, **101**, 396–403.
4 F. Miomandre, P. Audebert, M. Maumy and L. Uhl, *J. Electroanal. Chem.*, 2001, **516**, 66; I. A. Salem, M. Y. Elsheikh, A. B. Zaki and U. Nickel, *Int. J. Chem. Kinet.*, 1994, **26**, 955–962; H. V. Singh and Kamaluddin, *Oxid. Commun.*, 1995, **18**, 275; A. Bottcher, M. W. Grinstaff, J. A. Labinger and H. B. Gray, *J. Mol. Catal. A: Chem.*, 1996, **113**, 191; H. Tonami, H. Uyama, S. Kobayashi, H. Higashimura and T. Oguchi, *J. Macromol. Sci., Part A: Pure Appl. Chem.*, 1999, **A36**, 719; S. Kobayashi, H. Uyama and S. Kimura, *Chem. Rev.*, 2001, **101**, 3793; S. K. Edulji and S. T. Nguyen, *Organometallics*, 2003, **22**, 3374; R. B. Bedford, D. W. Bruce, R. M. Frost, J. W. Goodby and M. Hird, *Chem. Commun.*, 2004, 2822; K. P. Bryliakov and E. P. Talsi, *Angew. Chem., Int. Ed.*, 2004, **43**, 5228; H. Tonami, H. Uyama and S. Kobayashi, *Macromolecules*, 2004, **37**, 7901; G. A. Luinstra, G. R. Haas, F. Molnar, V. Bernhart, R. Eberhardt and B. Rieger, *Chem.–Eur. J.*, 2005, **11**, 6298; G. Hilt, C. Walter and P. Bolze, *Adv. Synth. Catal.*, 2006, **348**, 1241; K. P. Bryliakov and E. P. Talsi, *Chem.–Eur. J.*, 2007, **13**, 8045; G. Hilt, P. Bolze and K. Harms, *Chem.–Eur. J.*, 2007, **13**, 4312; G. C. Salomao, M. H. N. Olsen, V. Drago, C. Fernandes, L. C. Filho and O. A. C. Antunes, *Catal. Commun.*, 2007, **8**, 69; B. B. Fan, H. Y. Li, W. B. Fan, C. Jin and R. F. Li, *Appl. Catal., A*, 2008, **340**, 67; K. C. Gupta and A. K. Sutar, *Coord. Chem. Rev.*, 2008, **252**, 1420.
5 Y. W. Liou and C. M. Wang, *J. Electroanal. Chem.*, 2000, **481**, 102.
6 L. Q. Mao, K. Yamamoto, W. L. Zhou and L. T. Jin, *Electroanalysis*, 2000, **12**, 72.
7 C. Floriani, G. Fachinetti and J. Calderazzo, *J. Chem. Soc., Dalton Trans.*, 1973, 765; P. C. Ford and S. Wecksler, *Coord. Chem. Rev.*, 2005, **249**, 1382.
8 F. H. Allen, *Acta Crystallogr., Sect. B: Struct. Sci.*, 2002, **B58**, 380.
9 M. Gerloch, E. D. McKenzie and A. D. C. Towl, *J. Chem. Soc. A*, 1969, 2850.
10 W. J. Ruan, G. H. Hu, S. J. Wang, J. H. Tian, Q. L. Wang and Z. A. Zhu, *Chin. J. Chem.*, 2005, **23**, 709.
11 B. J. Kennedy, G. Brain, E. Horn, S. K. Murray and M. R. Snow, *Inorg. Chem.*, 1985, **24**, 1647; B. J. Kennedy, A. C. McGrath, K. S. Murray, B. W. Skelton and A. H. White, *Inorg. Chem.*, 1987, **26**, 483.
12 M. M. Bhadbhade and D. Srinivas, *Polyhedron*, 1998, **17**, 2699.
13 X. Wang, E. B. Sundberg, L. Li, K. A. Kantardjieff, S. R. Herron, M. Lim and P. C. Ford, *Chem. Commun.*, 2005, 477; B. O. Patrick, W. M. Reiff, V. Sanchez, A. Storr and R. C. Thompson, *Inorg. Chem.*, 2004, **43**, 2330; S. J. Rettig, A. Storr, D. A. Summers, R. C. Thompson and J. Trotter, *J. Am. Chem. Soc.*, 1997, **119**, 8675; Y. Naruta, N. Sawada and M. Tadokoro, *Chem. Lett.*, 1994, 1713.
14 Y. X. Gao, L. B. Wang and X. R. Hao, *Acta Crystallogr., Sect. E: Struct. Rep. Online*, 2007, **63**, m2232.
15 J. Tabernor, L. F. Jones, S. L. Heath, C. Muryn, G. Aromi, J. Ribas, E. K. Brechin and D. Collison, *Dalton Trans.*, 2004, 975; D. M. Low, L. F. Jones, A. Bell, E. K. Brechin, T. Mallah, E. Riviere, S. J. Teat and E. J. L. McInnes, *Angew. Chem., Int. Ed.*, 2003, **42**, 3781; R. Shaw, R. H. Laye, L. F. Jones, D. M. Low, C. Talbot-Eeckelaers, Q. Wei, C. J. Milios, S. Teat, M. Helliwell, J. Raftery, M. Evangelisti, M. Affronte, D. Collison, E. K. Brechin and E. J. L. McInnes, *Inorg. Chem.*, 2007, **46**, 4968.
16 G. Liu, A. M. Arif, F. W. Bruenger and S. C. Miller, *Inorg. Chim. Acta*, 1999, **287**, 109.
17 D. J. Price, S. R. Batten, B. Moubaraki and K. S. Murray, *Indian J. Chem., Sect. A: Inorg., Bio-inorg., Phys., Theor. Anal. Chem.*, 2003, **42**, 2256; Q. Shi, R. Cao, X. Li, J. H. Luo, M. C. Hong and Z. N. Chen, *New J. Chem.*, 2002, **26**, 1397.

18 J. S. Miller and A. J. Epstein, *MRS Bull.*, 2000, **25**, 21; C. Coulon, H. Miyasaka and R. Clerac, in *Single-Molecule Magnets and Related Phenomena*, ed. D. M. P. Mingos, 2006, vol. 122, pp. 163.
19 R. Guilard, I. Perrot, A. Tabard, P. Richard, C. Lecomte, H. Y. Liu and K. M. Kadish, *Inorg. Chem.*, 1991, **30**, 27.
20 P. Gütlich and J Ensling, Mössbauer spectroscopy, in *Inorganic Electronic Structure and Spectroscopy. Volume I. Methodology*, E. I. Solomon and A. B. P. Lever (Eds.), Wiley-Interscience, New York, 1999.
21 C. T. Brewer, G. Brewer, G. B. Jameson, P. Kamaras, L. May and M. Rapta, *J. Chem. Soc., Dalton Trans.*, 1995, 37.
22 N. N. Greenwood, T. C. Gibb, in *Mössbauer Spectroscopy*, Chapman and Hall Ltd, London, 1971.
23 M. E. Fisher, *Am. J. Phys.*, 1964, **32**, 343.
24 D. V. Lide, *The 84th Edition of the CRC Handbook of Chemistry and Physics*, CRC Press, 2004.
25 O. Kahn, *Molecular magnetism*, Wiley-VCH, New York, 1993.
26 O. Waldmann, *Phys. Rev. B: Condens. Matter Mater. Phys.*, 2000, **61**, 6138.
27 R. Boča, *Theoretical Foundations of Molecular Magnetism*, Elsevier, Amsterdam, 1999.
28 B. Kwak, K. W. Cho, M. Pyo and M. S. Lah, *Inorg. Chim. Acta*, 1999, **290**, 21.
29 I. Fridovich, *Annu. Rev. Biochem.*, 1995, **64**, 97; I. Fridovich, *J. Biol. Chem.*, 1989, **264**, 7761.
30 T. Matsushita and T. Shono, *Bull. Chem. Soc. Jpn.*, 1981, **54**, 3743.
31 B. J. Wallar and J. D. Lipscomb, *Chem. Rev.*, 1996, **96**, 2625.
32 T. Nagano, T. Hirano and M. Hirobe, *J. Biol. Chem.*, 1989, **264**, 9243.
33 S. Pervaiz and M. V. Clement, *Int. J. Biochem. Cell Biol.*, 2007, **39**, 1297.
34 M. V. Clement, A. Ponton and S. Pervaiz, *FEBS Lett.*, 1998, **440**, 13.
35 A. S. Kumbhar, S. G. Damle, S. T. Dasgupta, S. Y. Rane and A. S. Kumbhar, *J. Chem. Res. (S)*, 1999, 98; A. Silvestri, G. Barone, G. Ruisi, M. T. Lo Giudice and S. Tumminello, *J. Inorg. Biochem.*, 2004, **98**, 589.
36 P.C. Dedon, *Chem. Res. Toxicol.*, 2008, **21**, 206and the references therein.
37 S. Toyokuni, *Redox Rep.*, 2002, **7**, 189.
38 G. A. Woldemariam and S. S. Mandal, *J. Inorg. Biochem.*, 2008, **102**, 740; T. S. Lange, K. K. Kim, R. K. Singh, R. M. Strongin, C. K. McCourt and L. Brard, *PLoS One*, 2008, **3**, e2303.
39 P. D. Walker and S. V. Shah, *Kidney Int.*, 1991, **40**, 891.
40 K.I. Ansari, J. D. Grant, G. A. Woldemariam, S. K. Mandal and S. S. Mandal, *Org. Biomol. Chem.*, 2009, **7**, 926.
41 G.M. Sheldrick, *Acta Crystallogr., Sect. A: Found. Crystallogr.*, 1990, **46**, 467.
42 K. Brandenburg, *Diamond (Release 3.1e)*, Grystal Impact GbR, Bonn, Germany, 2006.
43 Z. Travnicek, M. Malon, M. Biler, M. Hajduch, P. Broz, K. Dolezal, J. Holub, V. Krystof and M. Strnad, *Transition Met. Chem.*, 2000, **25**, 265.

